International Journal of Thermophysics, Vol. 20, No. 4, 1999

Thermophysical Properties of the Zr–0.01Nb Alloy at Various Heating Rates and Repeated Cycles of Heating–Cooling[1]

I. I. Petrova,[2,3] V. E. Peletsky,[2] and B. N. Samsonov[2]

The results of an experimental study of the heat capacity, enthalpy, electrical resistivity, and spectral emissivity (for the wavelength of 0.65 μm) of the Zr–0.01Nb alloy in the temperature range from 900 to 2000 K are presented. The study was carried out using subsecond pulse heating of the samples by passing electrical current through them. Experiments were conducted at different heating rates (10^3 to 10^4 K $\cdot$ s^{-1}), and a series of experiments consisted of several cycles of pulse heating and subsequent cooling. The effect of these parameters on the temperature dependence of thermophysical properties in the region of the α–β transition was studied. With an increase in the heating rate, the temperature of the α–β transition, and the maximum in the heat capacity shifted to higher temperatures. There are significant differences in properties over the temperature range of the α–β transition for the various heating cycles.

KEY WORDS: α–β transition; electrical resistivity; enthalpy; heat capacity; melting temperature; spectral emissivity; subsecond pulse heating technique; zirconium alloy.

1. INTRODUCTION

Zirconium alloys are used for the envelopes of fuel elements and other parts of nuclear reactors. Reliable data on the thermophysical properties of these alloys at high temperatures are necessary to predict the behavior of the envelopes of fuel elements under accident conditions, when their temperatures increase abruptly and can reach melting.

---

[1] Paper presented at the Fifth International Workshop on Subsecond Thermophysics, June 16–19, 1998, Aix-en-Provence, France.

[2] High Energy Density Research Center, Institute for High Temperatures, Izhorskaya 13/19, 127412 Moscow, Russia.

[3] To whom correspondence should be addressed.

There are insufficient data for the thermophysical properties of Zr alloys in the literature, Zircalloy-2 (Zr–0.015Sn) has been the alloy studied most [1–3]. Data on thermophysical properties of the Zr–0.01Nb alloy are practically nonexistent. However, it is known that different alloy compositions as well as impurities exert a great influence on properties, especially in the region of the α–β phase transition.

Recently [4, 5] we have measured the thermophysical properties of the Zr–0.01Nb alloy in the temperature range from 500 K up to melting using thermocouples, which can result in significant errors in temperature measurements due to signal delays of response and to the voltage drop between the points of thermoelectrode contacts. They are caused by the conditions of rapid heating when large electric currents pass through the specimen.

In this work with the new pyrometer, which has a lower limit of measurement of 900 K, we were able to study the region of the α–β phase transition in detail and, in particular, to investigate the influence of the heating rate and repeated cycles of heating–cooling on the behavior of the temperature dependence of the thermophysical properties in this region.

2. MEASUREMENTS

2.1. Principle of Measurement

As is well known, zirconium and its alloys actively absorb gases from the environment, especially at high temperatures. If the samples are held at high temperatures for a long time, their chemical composition can change, which, in turn, can influence thermophysical properties, especially in the region of the solid–solid α–β phase transition, where anomalous changes of properties occur. So the classical steady-state methods are not suitable for measurements of thermophysical properties. The method of subsecond pulse-resistive self-heating allows us to overcome these difficulties, i.e., to conserve the initial chemical composition of the samples as a result of the short (about 1 s) times of heating and comparatively short periods of cooling.

During heating, the values of a direct current I passed through the sample, the voltage drop U on the central measured section of the sample, the true temperature T_{tr}, and the brightness temperature T_{br} of the sample are measured as a function of time τ. Using these parameters, the enthalpy H_t–$H_{298\,\mathrm{K}}$, the heat capacity C_{p}, the spectral (for wavelength of 0.65 μm) emissivity ε_λ, and the electrical resistivity ρ can be calculated with the following equations:

$$C_p = \frac{UI - q_r}{m(dT/d\tau)_h} \tag{1}$$

$$H_t - H_{298\,\mathrm{K}} = \frac{1}{m} \int_0^{\tau} (UI - q_r)\, d\tau \tag{2}$$

$$\ln \varepsilon_\lambda = \frac{c_2}{\lambda} \left(\frac{1}{T_{tr}} - \frac{1}{T_{br}} \right) \tag{3}$$

$$\rho = \frac{U}{I} \frac{S}{l} \tag{4}$$

In these expressions m is the mass of the central working section of the sample, $C_2 = 1.4388 \times 10^{-2}\ \mathrm{m \cdot K}$ is the second constant in Planck's law, S is the cross-sectional area of the sample, l is the length of the central section of the sample, $(dT/d\tau)_h$ is the rate of heating of the sample, and q_r is a correction for the radiation heat losses.

2.2. Method of Measurement

A schematic diagram of the measurement method is shown in Fig. 1. The sample is heated by a source of direct current (a three-phase rectifier with an output voltage of 15 or 30 V), which provides a current pulse up

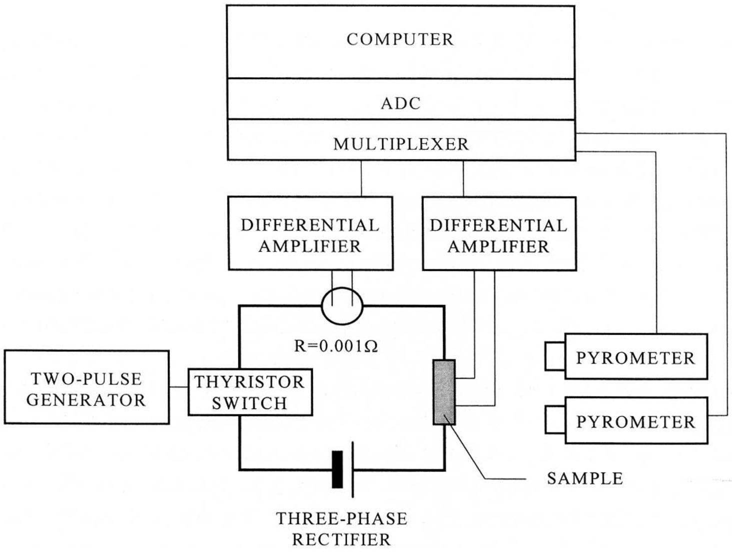

Fig. 1. Schematic diagram of the measurement technique.

to 1500 A. The circuit of the sample is closed by a thyristor switch. The pulse duration is set with a two-pulse generator. A standard resistor ($R = 0.001\ \Omega$) is used for measurements of the electrical current in the circuit. Two high-speed photoelectric pyrometers (wavelengths of 0.65 μm) measure the temperatures of the sample during heating and subsequent cooling. One of the pyrometers measures the brightness temperature of the surface (its lower limit of measurements is about 1600 K), and the other one measures the true temperature in the blackbody model (its lower limit is 900 K). Pyrometers have been calibrated with a reference temperature tungsten strip lamp placed in the chamber instead of the sample in order to exclude errors associated with possible overlapping of radiation flow from the sample and to exclude determination of the transmission of the glasses in the chamber windows. All primary parameters are measured using an A/D converter with a multiplexer and collected in the memory of a computer for further processing. The electrical current and the voltage drop are measured using the differential amplifiers. The frequency of measurement cycles for four parameters (U, I, T_{tr}, T_{br}) is given by the program and is usually equal to 10^3 Hz.

2.3. Samples

For this investigation of the thermophysical properties of the Zr–0.01Nb alloy, samples of tubular and strip forms made of industrial fuel element envelopes were used. The length of the tubular samples was 75 mm; the distance between two probes in the central part of the sample, where the voltage drop was measured, was 10 mm; the outer diameter of the tube was 9.15 mm; and the wall thickness was 0.65 mm. The blackbody model for measurement of the true temperature was made with a rectangular slit, 20 mm long and 1 mm wide. The effective emissivity for such a blackbody was found experimentally and was equal to 0.89 [6]. Strip samples were 75 mm long, 6 mm wide, and 0.65 mm thick. The distance between probes was also 10 mm. In the experiments with strip samples, the true temperature was calculated using the measured brightness temperature and recommended data [7] on the spectral emissivity ε_λ of zirconium. Using samples in two forms—tubes and strips—enabled us to perform experiments at different heating rates. To determine the influence of multiple cycles of heating–cooling on the thermophysical properties of a Zr–0.01Nb alloy, a series of pulse experiments was carried out on the same sample. The experiments were performed in an argon atmosphere at a pressure of 1.1×10^5 Pa. The chemical composition of the samples is given in Ref. 5.

The initial structure of the samples consists mainly of the α-Zr phase (α-Zr with dissolved Nb), with a small quantity of very small particles of the β-Nb phase (β-Nb with dissolved Zr).

3. RESULTS

3.1. Influence of Heating–Cooling Cycles

Four experiments (pulse heating-subsequent cooling), with 30-min intervals between them, were performed on the tubular samples. The heating rate was about 1.3 to $1.5 \times 10^3\ \mathrm{K \cdot s^{-1}}$, and the cooling rate at the initial stage was about $200\ \mathrm{K \cdot s^{-1}}$. For the first three pulses the heating period was set to 1.3 s. In this case the highest temperature of the sample was about 1900 K. For the fourth pulse, the heating period was increased and the sample became molten. Figure 2 shows the dependences of $T_{\mathrm{tr}} = f(\tau)$, which have been measured for these four experiments on the same sample. It may be seen that the results of the first experiment differ appreciably from the following ones. The plateau of the α–β transition for the first pulse is more apparent and longer than for the others.

Differences between the thermograms of heating for the first experiment and the following ones can be explained by the fact that after the first heating pulse, the sample cooled down rapidly (its cooling rate was about $200\ \mathrm{K \cdot s^{-1}}$) and its structure after cooling differed from the initial structure.

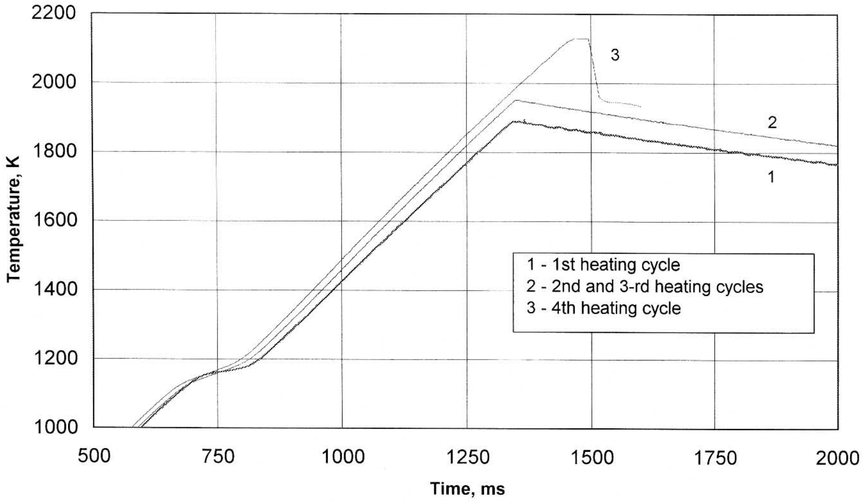

Fig. 2. True temperature thermograms for four experiments on the same tubular sample.

As the electron micrograph analysis showed after the first experiment, the sample consisted of the metastable α' phase (supersaturated solution of Nb in α-zirconium) of acicular martensitic type. It appeared again after every new experiment.

To determine the temperature range of the α–β phase transition, the time dependences of resistivity $\rho = f(\tau)$ and corresponding thermograms $T_{\mathrm{tr}} = f(\tau)$ were used. Figure 3 shows how the conventional temperatures at the beginning ($T^{\alpha}_{\rho_{\mathrm{max}}}$) and end ($T^{\beta}_{\rho_{\mathrm{min}}}$) of the α–β phase transition were determined using the maximum value of resistivity in the α phase ($\rho^{\alpha}_{\mathrm{max}}$) and the minimum in the β phase ($\rho^{\beta}_{\mathrm{min}}$). As may be seen from Fig. 3, these conventional values differ from the values which can be obtained on the basis of the thermogram $T_{\mathrm{tr}}(\tau)$. The reason for this difference needs to be understood.

Table I gives the temperatures of the beginning and the end of the α–β phase transition and temperature ranges $\Delta T^{\rho}_{\alpha\text{-}\beta}$ of the transition, as well as the maximum and minimum values of resistivity and their ratio for four successive heating pulses on the same sample. The temperature range of the α–β phase transition for the first heating period is 80 K, which was less than for the following ones (140, 125, and 115 K). This behavior is also explained by the appearance of a new metastable α' phase during rapid cooling of the sample at a rate of about $200\ \mathrm{K \cdot s^{-1}}$ after the first and following heating cycles.

The enthalpy of phase transition $\Delta H_{\alpha\text{-}\beta}$ was determined from $\rho = f(H)$ dependence as the difference in enthalpy values at the points where

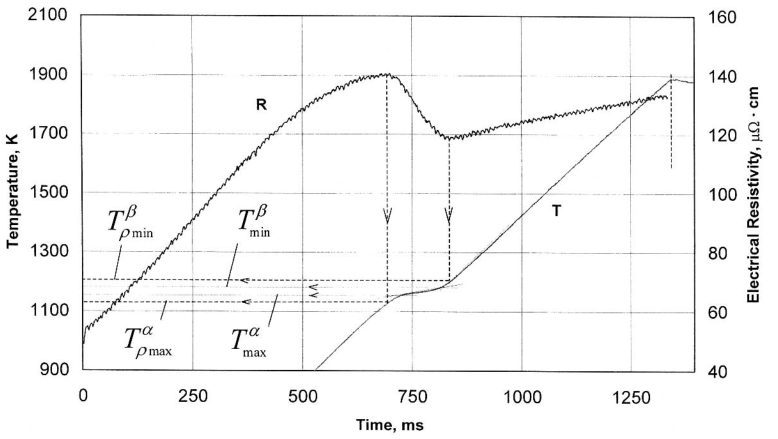

Fig. 3. Determination of the beginning and the end of the phase transition based on the measurement of $\rho(\tau)$ and $T(\tau)$.

Table I. Thermophysical Properties of the Zr-0.01Nb Alloy in the Region of the α–β Transition for Repeated Heating Cycles

	1st pulse	2nd pulse	3rd pulse	4th pulse
$\rho^{\alpha}_{\max}(\mu\Omega\cdot\mathrm{cm})$	140	139	140	139
$\rho^{\beta}_{\min}(\mu\Omega\cdot\mathrm{cm})$	118	120	120	120
$\rho^{\alpha}_{\max}/\rho^{\beta}_{\min}$	1.186	1.158	1.167	1.158
$T^{\alpha}_{\rho\,\max}(\mathrm{K})$	1120	1070	1085	1100
$T^{\beta}_{\rho\,\min}(\mathrm{K})$	1200	1210	1210	1215
$\Delta T^{\rho}_{\alpha\text{-}\beta}(\mathrm{K})$	80	140	125	115
$H^{\alpha}_{\max}\,(\mathrm{J\cdot g^{-1}})$	275	255	260	265
$H^{\beta}_{\min}\,(\mathrm{J\cdot g^{-1}})$	345	345	345	345
$\Delta H_{\alpha\text{-}\beta}(\mathrm{J\cdot g^{-1}})$	70	90	85	80
$\Delta\tau_{\alpha\text{-}\beta}(\mathrm{ms})$	150	180	180	160

resistivity has its maximum in the α phase and its minimum in the β phase. The enthalpy at the beginning of the transition in the first experiment ($H^{\alpha}_{\max} = 275\ \mathrm{J\cdot g^{-1}}$) is larger than for the other three. The enthalpy at the end of the transition is the same for all experiments ($H^{\beta}_{\min} = 345\ \mathrm{J\cdot g^{-1}}$). The enthalpy of the phase transition for the first experiment ($\Delta H_{\alpha\text{-}\beta} = 70\ \mathrm{J\cdot g^{-1}}$) is less than in the following heating cycles (average value of $\Delta H_{\alpha\text{-}\beta}$ for the second, third, and fourth experiments is $85\ \mathrm{J\cdot g^{-1}}$). In Table I we present the results for the enthalpy of the α–β phase transition for four successive heat pulses and periods of the phase transition $\Delta\tau_{\alpha\text{-}\beta}$.

The spectral (for $\lambda = 0.65\ \mu\mathrm{m}$) emissivity ε_{λ} of the Zr-0.01Nb alloy was calculated using the true and brightness temperature values obtained during pulse heating. For the first heating cycle, ε_{λ} changes from 0.55 to 0.48 in the temperature range from 1700 to 1900 K. For the next three experiments, the behavior of ε_{λ} is identical and changes from 0.490 to 0.425 over the temperature range of 1700 to 2100 K. Higher values of ε_{λ} for the first experiment are probably connected with the formation of oxide film on the surface of the sample during the initial stage of heating due to oxygen absorbed before the experiment when the vacuum chamber was open. Because of the diffusion of oxygen from the oxide film into the metal at high temperatures during the final stage of the first heating, and especially during the initial stage of the subsequent longer cooling period, the oxide film disappears from the surface and ε_{λ} decreases.

Figure 4 shows the results of the heat capacity measurements. For the α and β phases, the values of C_p, obtained for all experiments, are practically the same. Differences in the structure of the α' and α phases do not

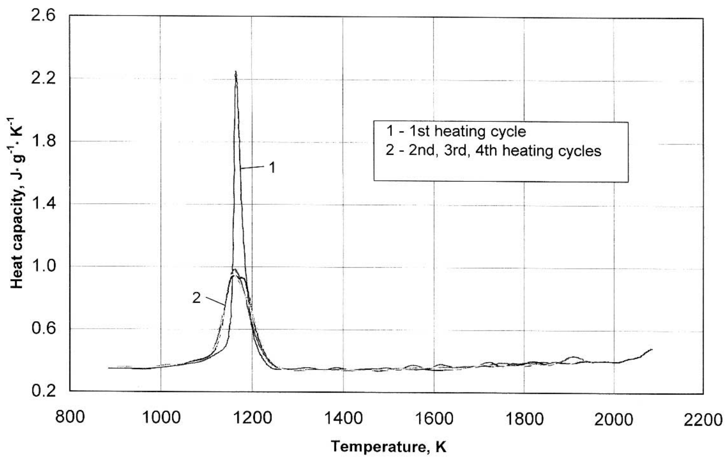

Fig. 4. Heat capacity measured for four experiments with the same sample.

influence the thermophysical properties at temperatures below the temperature of the phase transition. However, over the range of the α–β phase transition, there is a large difference. The heat capacity peak for the first experiment reaches $2.3\ \mathrm{J \cdot g^{-1} \cdot K^{-1}}$; for the other experiments it is equal to approximately $0.95\ \mathrm{J \cdot g^{-1} \cdot K^{-1}}$. For the first heating period the peak of $C_p(T)$ is narrower than for the others. Probably, the small particles of the β-Nb phase, which are present in the sample structure before the first heating, act as nuclei of the β phase at the α–β phase transition.

For the β phase in the temperature range of 1250 to 2000 K, the heat capacity (in $\mathrm{J \cdot g^{-1} \cdot K^{-1}}$) can be approximated as follows:

$$C_p = 0.6448 - 0.4558 \times 10^{-3} T + 0.1713 \times 10^{-6} T^2 \qquad (5)$$

3.2. Influence of Heating Rate on Thermophysical Properties

To determine the influence of the heating rate on the thermophysical properties of the Zr–0.01Nb alloy, experiments on tubular and strip samples were performed. Heating rates were as follows: for tubes at the source voltages of 15 and 30 V, 1.3 to 1.5×10^3 and 2.5 to $2.8 \times 10^3\ \mathrm{K \cdot s^{-1}}$, respectively; and for strips, 5 to 7×10^3 and 1 to $1.4 \times 10^4\ \mathrm{K \cdot s^{-1}}$. It was noted that as the heating rate rises from 10^3 to $10^4\ \mathrm{K \cdot s^{-1}}$, the temperature of the phase transifion (temperature in the middle of the plateau) shifts to higher values: from 1160 to 1230 K.

Figure 5 shows the results for the heat capacity from 1000 K up to melting obtained at different heating rates. All experiments were performed

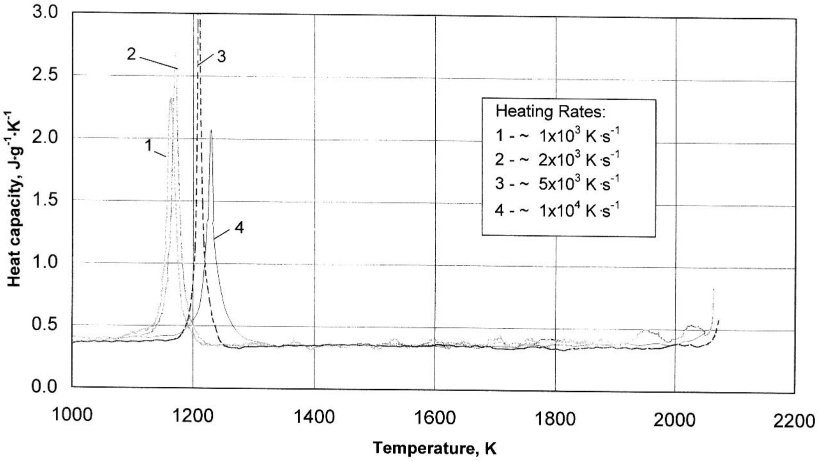

Fig. 5. Heat capacity of the Zr–0.01Nb alloy at different heating rates.

on samples of the same initial composition and structure. It is noticeable that the heat capacity in the α and β phases does not depend on the heating rate. In the region of the α–β transition, the peak in the heat capacity shifts from 1160 to 1230 K with an increase in the heating rate, and its magnitude changes.

The shift in temperatures of the α–β transition for rapid heating relative to the equilibrium value can be obtained by comparison with the known phase diagram [8] of the Zr–Nb system. The known temperatures of the beginning and the end of the equilibrium phase transition are 893 and 1135 K, respectively [8]. However, the magnitudes of the shifts, obtained on the basis of the dependence of $\rho(\tau)$ and corresponding dependence $T=f(\tau)$ for the same experiment, are different, as mentioned above. For example, for a heating rate of $\sim 10^3\ \mathrm{K\cdot s^{-1}}$, the temperature at the beginning of the α–β phase transition, determined from the dependence $\rho=f(\tau)$, is 1120 K. The plateau on the thermogram $T=f(\tau)$ for the same experiment appears at $T=1150$ K, i.e., the temperature difference is about 30 K. At a heating rate of $\sim 10^4\ \mathrm{K\cdot s^{-1}}$, this difference is about 60 K. The differences in temperatures of the end of the phase transition for different heating rates by the two methods noted above are less.

3.3. Estimation of Errors

The errors of measurements have been estimated using the method described in Ref. 9. The total (systematic + random) errors in determination of the heat capacity, enthalpy, electrical resistivity, and spectral emissivity over the whole temperature range excluding the region of the α–β phase transition do not exceed 3.5, 2.2, 1.5, and 3.5%, respectively. The total errors in determination of the electrical resistivity and heat capacity in the temperature region of the α–β phase transition are much higher. The error for the heat capacity can reach 10 to 12%.

4. CONCLUSION

It is determined that the influence of the heating rate on the thermophysical properties of the Zr–0.01Nb alloy has vital importance in the temperature region of the α–β phase transition. When the heating rate increases, the temperature at the beginning of the α–β phase transition shifts to higher values relative to the equilibrium one. This shift is about 230 K at a heating rate of $10^3\ \mathrm{K \cdot s^{-1}}$ and about 280 K at $10^4\ \mathrm{K \cdot s^{-1}}$. The differences in temperatures at the end of this transition are much less.

When the heating rate increases from 10^3 to $10^4\ \mathrm{K \cdot s^{-1}}$, the peak in the heat capacity shifts from 1160 to 1230 K. The heating rate does not affect the thermophysical properties in either the α-phase or the β-phase temperature region.

The experiments, performed for determination of the effect of pulse heating–cooling cycles on thermophysical properties, showed that for the first experiment, when the specimen had initial structure before heating, the peak of the heat capacity was double its value for the following heating cycles. The temperature range of the α–β phase transition for the first heating was less than for the following ones. This is explained by the appearance of the new metastable α' phase during the rapid cooling of the sample at a rate of about $200\ \mathrm{K \cdot s^{-1}}$.

The cycles of heating–cooling have no effect on the thermophysical properties in the temperature regions of the α and β phases. The difference in the structures of the α' and α phases does not influence the thermophysical properties.

REFERENCES

1. F. Righini, A. Rosso, and L. Coslovi, in *Proc. Seventh Symp. Thermophys. Prop.*, A. Cezairliyan, ed. (ASME, New York, 1977), p. 358.
2. F. Righini, L. Coslovi, and A. Rosso, in *Proc. Eighth Symp. Thermophys. Prop.*, J. V. Sengers, ed. (ASME, New York, 1981), p. 51.
3. K. D. Maglic, N. L. Perovic, and A. M. Stanimirovic, *Int. J. Thermophys.* **15**:741 (1994).
4. V. E. Lusternik, V. E. Peletsky, and I. I. Petrova, *High Temp.-High Press.* **25**:539 (1993).
5. V. E. Peletsky and I. I. Petrova, *High Temp.-High Press.* **29**:373 (1997).

6. I. I. Petrova and V. E. Peletsky, *High Temp.* **33**:710 (1995).
7. L. N. Latyev, V. A. Petrov, V. Ya. Chechovskoy, and E. N. Shestakov, in *Izluchatelnye svoystva tverdykh materialov (Thermal Radiation Properties of Solid Materials)*, A. E. Sheindlin, ed. (Energia, Moskva, 1974), p. 264.
8. A. F. Guillermet, *Z. Matallkde* **82**:478 (1991).
9. S. G. Rabinovitch, *Metrologia* **3**:3 (1970).